NOTES AND CORRESPONDENCE

Global Ocean Warming: An Acoustic Measure?

W. H. MUNK

Institute of Geophysics & Planetary Physics, Scripps Institution of Oceanography, University of California, San Diego, La Jolla, California

A. M. G. FORBES

CSIRO Division Oceanography, Hobart, Tasmania 7, Australia

6 February 1989 and 11 May 1989

ABSTRACT

Explosions of 300 lbs of TNT at 1 km depth off Perth, Australia were recorded on Bermuda hydrophones, demonstrating 30 years ago the feasibility of global acoustic transmissions. Climate-induced changes in ocean temperature (and hence in sound speed) can be monitored by measuring travel time changes of acoustic signals from remote powerful sources. Warming induced now at the sound axis by CO_2 and other greenhouse gases is estimated at 0.005°C per year, too small to be measured locally in the presence of 1°C rms noise from gyre scale and mesoscale fluctuations. The associated rate of decrease in travel time from greenhouse warming (a global measure of temperature rise) is estimated at 0.1 to 0.2 s per year. This climatic signal should be detectable above the gyre and mesoscale noise (less than 1 s rms), given a program of measurements carried out over a decade. An acoustic source at Heard Island in the south Indian Ocean has direct oceanic paths into all five ocean basins—westward to South Georgia, Brazil, South Africa and Bermuda; eastward to Tasmania, New Zealand, Tahiti, Hawaii, San Francisco and Oregon; northward to Indonesia and; southward to Antarctica. A feasibility experiment is planned.

1. Introduction

In 1960, 300 lbs of high explosives were detonated near the sound axis off Perth, Australia, and these were clearly recorded on axial hydrophones off Bermuda (Fig. 1). The results (not published until 1982) were interpreted as a nearly antipodal (179.2°) great-circle transmission (Shockley et al. 1982). But the shortest distance on an elliptical earth is the geodesic, and this differs considerably from the great circle path when the range is close to antipodal. The geodesic would be the proper ray path if the sound speed were uniform. But there are significant differences between the warm equatorial waters (fast sound speed) and the cold polar waters. Using data from about 8000 hydrographic stations (Fig. 2), the depth and sound speed of the axial ocean have been mapped (Munk et al. 1988) (Fig. 3). Rays follow the sound axis as it rises from 1 km depth at Perth to about 200 m in antarctic water and then descends to 1 km at midlatitudes, provided the transition is sufficiently gradual (Dashen and Munk 1984). The late near-axial arrivals (the SOFAR signal, see Fig. 10) are presumed to be the only ones to survive the very long transmission range. When allowance is made for the lateral gradients, particularly for the sharp decrease in sound speed from 40° to 60°S as the Antarctic Circumpolar Current is crossed, the constructed ray paths are dramatically altered. All paths are refracted southward towards the cold, slow polar water (Fig. 4). The refracted ray with the geodesic launch angle now intersects the South American continent. As the launch angle is rotated clockwise, rays clear the South American coast but pass to the south of Bermuda. With further rotation rays intersect the shallow Agulhas Bank off Cape of Good Hope but still miss Bermuda. Accordingly in this entire aperture between South America and South Africa (as seen from Perth) rays fail to intersect Bermuda; the island lies in the shadow.

But the acoustic signal *did* reach Bermuda. Estimates of various processes for refracting or scattering acoustic energy into the shadow zone lead to a reduction in intensity by one order of magnitude relative to the intensity in the illuminated region at similar ranges (Munk et al. 1988). The hypothesis (illustrated in Fig. 4) that the sound traveled along the refracted (solid) ray from Perth to Cape Agulhas, and from there along another refracted ray (heavy dashed) to Bermuda is strongly supported by the fact that the computed travel time is then within 2 s of the measured travel time of 13 382 s; in comparison, the travel time along the unrefracted geodesic is 50 s too long.[1]

Corresponding author address: Dr. Walter Munk, Instit. of Geophysics and Planetary Physics, Scripps Instit. of Oceanography, A-025, La Jolla, CA 92093.

[1] In April 1964, eighteen 50 pound explosive SUS charges were dropped on a flight from Capetown to Perth and recorded off New

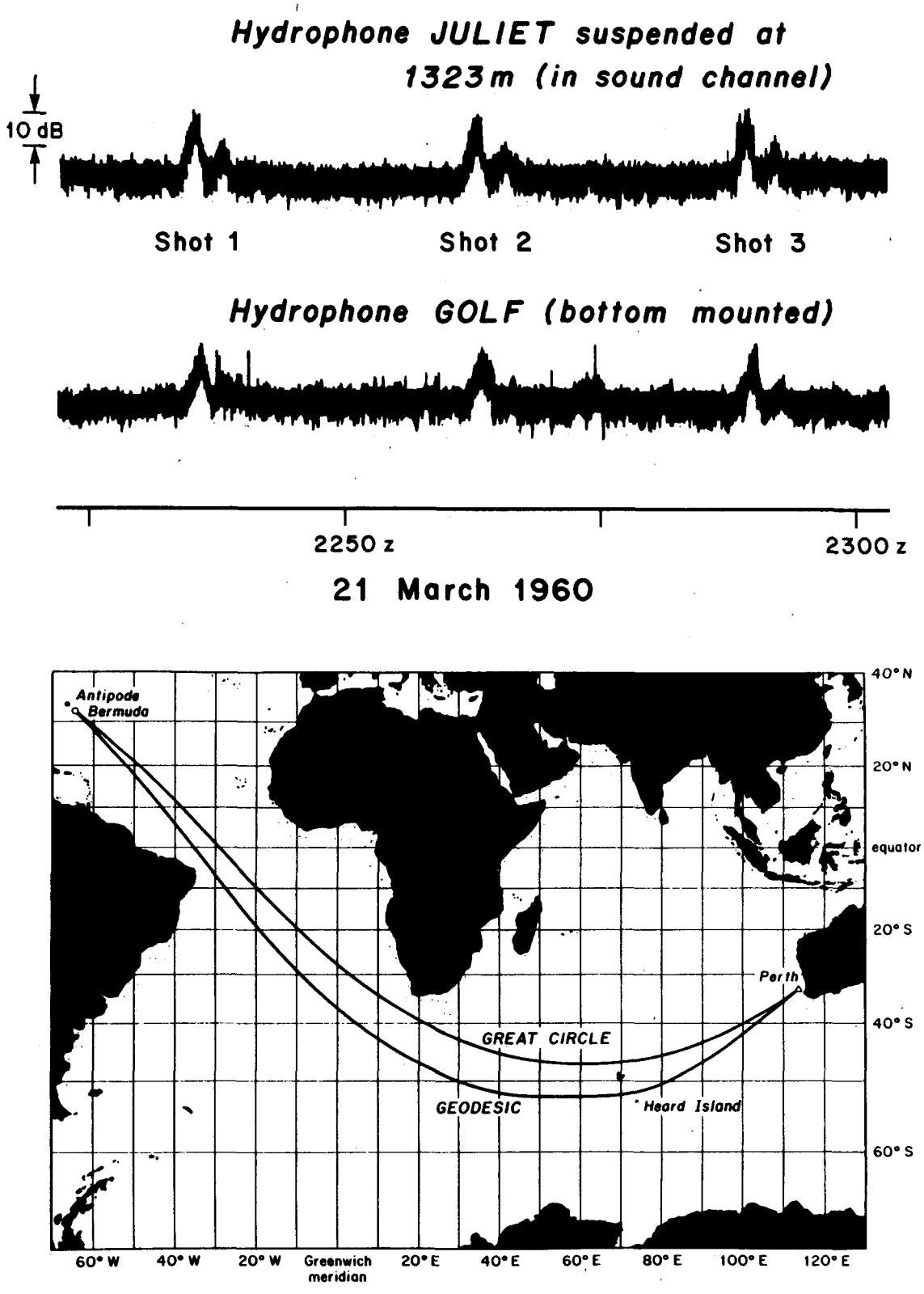

FIG. 1. The great circle and geodesic from the detonation site off Perth, Australia, to the hydrophones off Bermuda (Mercator projection). The angular range is 178°.2, just short of antipodal (180°). Top: reproduction of the original Bermuda records from three detonations (adapted from Shockley et al. 1982). Travel times were 3.7 hours.

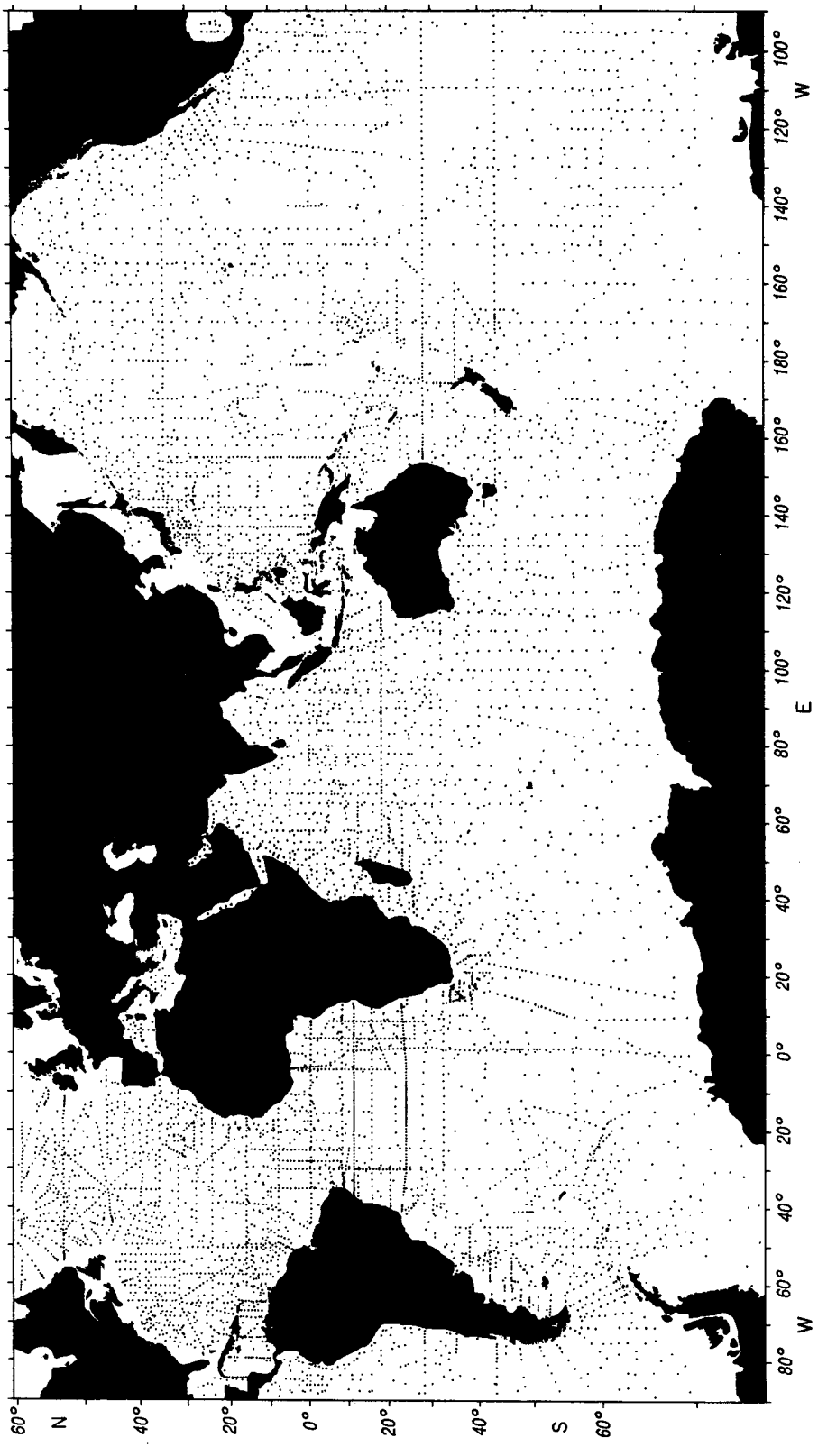

FIG. 2. Location of stations used for reconstructing the axial sound speed.

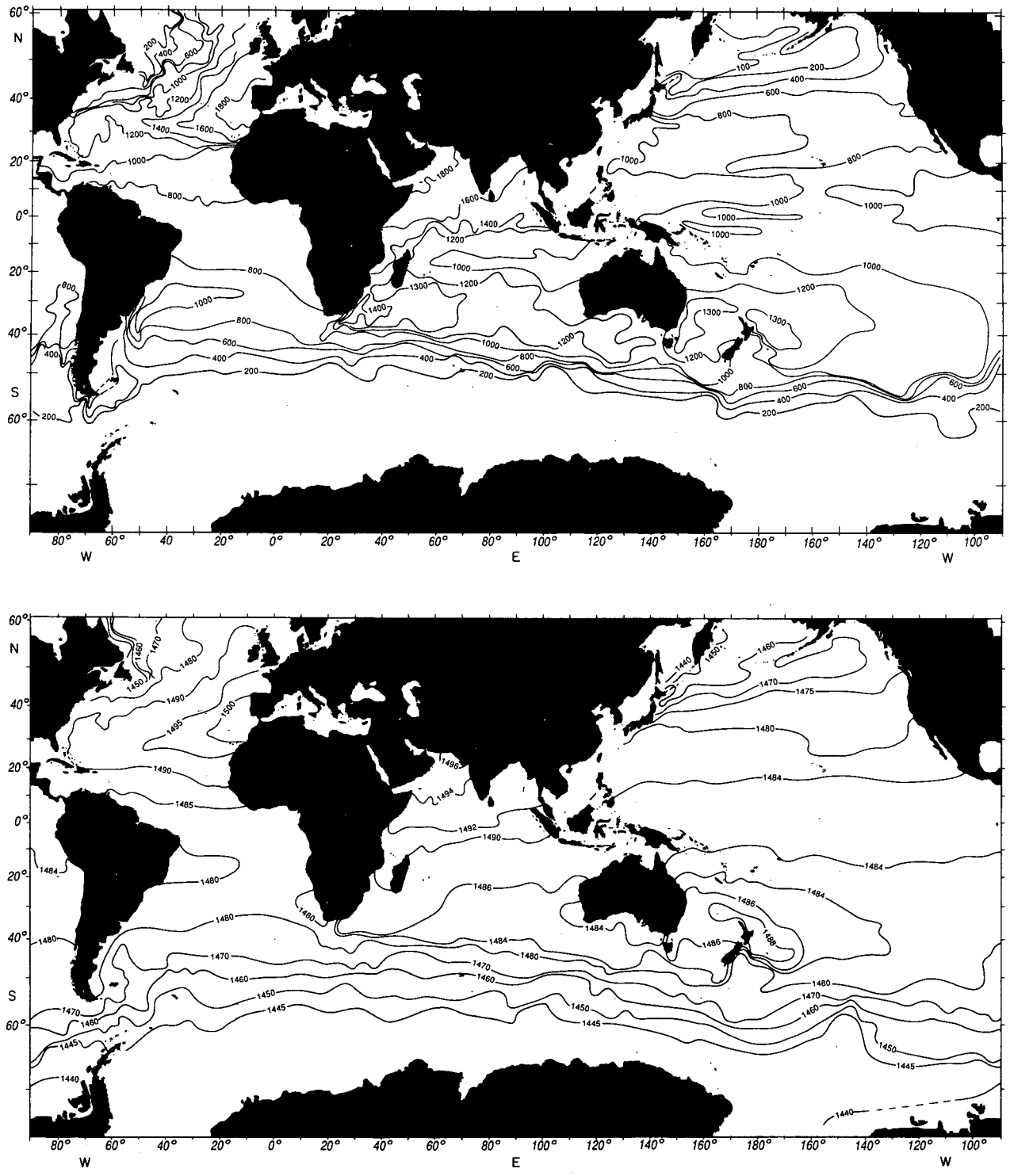

FIG. 3. The depth of the minimum sound speed axis in m (top), and the sound speed in m s^{-1} on the axial surface (bottom). The axis is at a typical midlatitude depth of order 1 km but outcrops at high northern and southern latitudes.

Zealand at ranges up to 10,000 km (Kibblewhite et al. 1965). One transmission passing just south of Heard Island was clearly received. The shot points are not accurately located, and it is not possible to reconstruct the events as could be done for the Perth transmission.

2. Heard Island

In looking for a source site farther south with direct access to Bermuda, we became aware of some unique

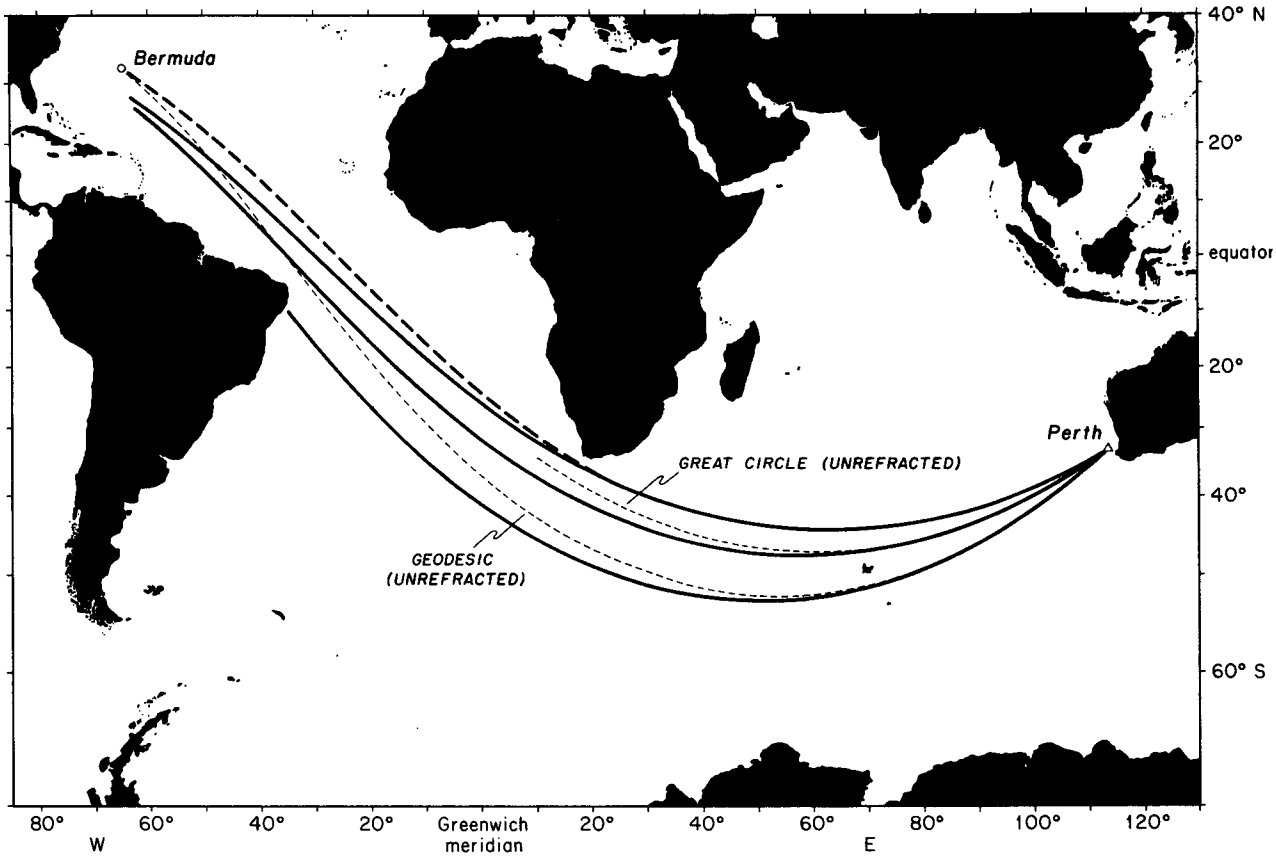

FIG. 4. Acoustic rays allowing for earth ellipticity and for lateral refraction (i.e. "refracted geodesics") from the sound speed gradients shown in Fig. 3. The ray with the geodesic launch angle at Perth is refracted southward and collides with Brazil. A clockwise rotation of the launch angle up to the ray which is tangent to Cape Agulhas (near the Cape of Good Hope) fails to intersect Bermuda, which lies in the geometric shadow. It is believed that the Perth-Bermuda transmission followed the refracted geodesic (heavy solid) from Perth to Cape Agulhas and another refracted geodesic (heavy dashed) from Cape Agulhas to Bermuda.

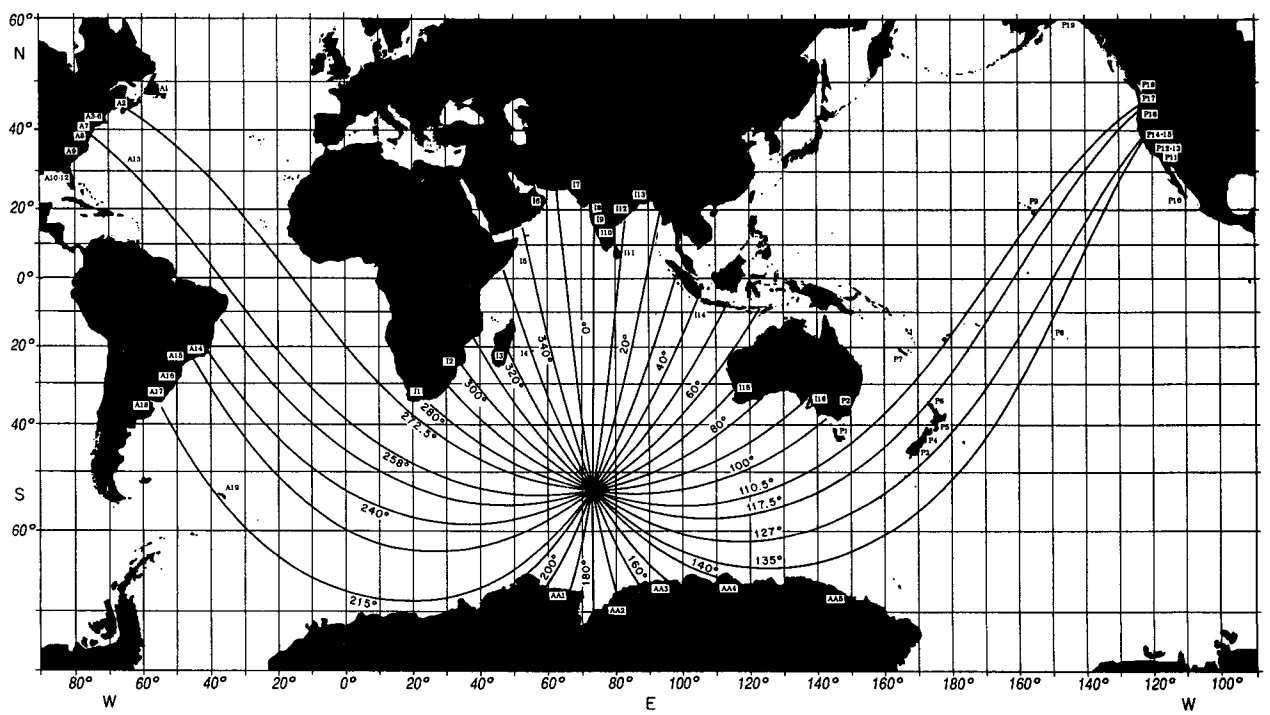

FIG. 5. Refracted rays (allowing for ellipticity) out of Heard Island, with indicated launch angles. There are unimpeded paths westward to Bermuda, and eastward to northern California, and to many other locations. White boxes indicated locations where oceanographic research stations are located.

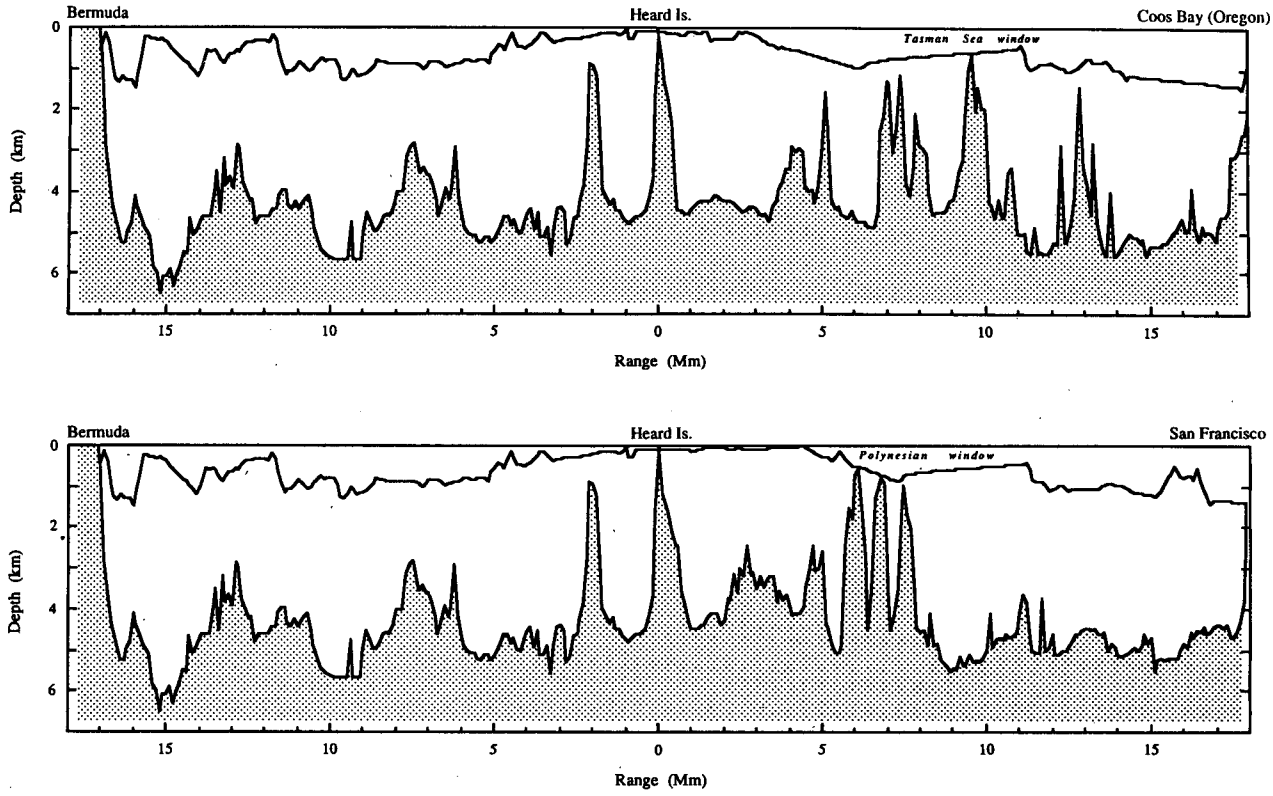

FIG. 6. Depth of bottom and sound channel along the ray paths shown in Fig. 5 from Heard to Bermuda (left), from Heard to Coos Bay (right top) and from Heard to San Francisco (right bottom).

advantages of the location of Heard Island in the south Indian Ocean. Not only is there an unimpeded westward refracted ray path to Bermuda, there is also a path eastward into the South Pacific reaching San Francisco, and possibly a path through the Tasman Sea reaching Coos Bay, Oregon (Figs. 5[2] and 6). Thus a source at Heard Island could be heard on both sides of North America—it could be heard off New Zealand, Tasmania, Perth, Indonesia, South Georgia, and the Indian Ocean sector of Antarctica—thus suggesting the possibility of monitoring climatic temperature changes by measuring acoustic travel times from a source off Heard Island to receivers at many locations. *Differential* travel time changes (e.g., Heard to Tasmania versus Heard to San Francisco) should provide evidence for changes in individual ocean basins. The suggestion is a natural outgrowth of the work on ocean acoustic tomography (Spindel and Spiesberger 1981; Munk and Wunsch 1982; Munk and Worcester 1988; Knox 1988) for mapping the regional ocean temperature field. In both the regional and climatic application the underlying principle is that increasing temperature gives increasing sound speed and decreasing travel times.

3. The greenhouse effect

Nearly all modern investigations of the greenhouse effect are based on the measurements by Keeling starting in 1957, showing an increase in atmospheric CO_2 from 315 to 350 ppmv over a 25 year period (Mook et al. 1983; Keeling et al. 1984; Schlesinger 1986). The combined effect of the "greenhouse gases" (CO_2, methane and other trace constituents) is about twice that of CO_2 alone. The time scale of the combined atmosphere–ocean system to adjust to a sudden change in the greenhouse gases has been estimated between 10 and 100 years, and depends critically on ocean mixing processes. Actual observations of atmospheric surface warming are based on temperature time series at some 10^3 locations. They suffer from the fact that many of the land stations are contaminated by so called "urban heat islands" where the microclimate has undergone significant changes. Sea surface temperatures are contaminated by a systematic conversion from bucket to injection measurements: the bias so introduced may constitute as much as 50% of the observed change since the turn of the century (Barnett 1984a; Folland and Parker 1988). After attempting to correct for the biases,

[2] All rays are refracted geodesics along the surface containing the sound axis (Fig. 3 top). It is assumed that rays follow this surface adiabatically. The three-dimensional refraction problem is now being attempted by Semtner (personal communication).

various estimates suggest a surface warming (atmosphere and ocean) by 0.3 to 0.7°C.

Quite aside from these measurement problems, Barnett and Schlesinger (1987) have discussed the difficulty of detecting the global greenhouse warming against the background of the inherent air temperature variability. They find that greenhouse warming and inherent variability have similar spatial patterns, thus suggesting that the air temperature field is a difficult place to attempt early detection of the greenhouse signal. By contrast, they find that the expected greenhouse signal in the ocean is substantially different from the pattern of natural variability; accordingly the authors suggest that the oceans may be a better environment for early greenhouse detection.

We divide (somewhat arbitrarily) the discussion of acoustic detectability of ocean processes into three categories: the greenhouse effect, decadal variations and mesoscale variations. The greenhouse warming is our theme; others may find the mesoscale and decadal variations as their primary concern.

4. The greenhouse effect on ocean temperature

a. Numerical modeling

The simplest of these is a one-dimensional model in which the ocean mixing processes are parametrized in terms of a vertical diffusivity and an upwelling velocity (Hoffert et al. 1980). These parameters are adjusted to account for the vertical distributions of radiocarbon, inorganic carbon, alkalinity, dissolved oxygen and other geochemical tracers; the CO_2 increase scenario is from Wuebbles et al. (1984). The computed average (Table 1) of 3.0 m °C yr^{-1} (1 m °C = 0.001°C) is dominated by the relatively large rate of warming at the high southern latitudes where the sound channel is shallow. (We are indebted to V. Narayanan for carrying out the computations.)

The above estimates are for orientation only. Simulations by a coupled atmosphere–ocean circulation model (Schlesinger and Xingjian 1988) indicate a strong latitude dependence. Surface warming increases from the tropics towards the midlatitudes of both hemispheres, with greater depth penetration in the middle and high latitudes; in the tropics the penetration is minimized by the upwelling of cold water.

A coupled ocean–atmosphere GCM simulation (Bryan et al. 1988) emphasizes the asymmetry between the two hemispheres; in the Southern Hemisphere there is more deep warming and less shallow warming, with the total heat added being about the same in both hemispheres. Manabe, Spelman and Bryan (personal communication, designated in Table 1 by MSB) have calculated the warming along the specified coordinates of the Heard–Bermuda (16 Mm) and Heard–Coos Bay (18 Mm) transmission paths (1 Mm = 1000 km), using the coupled model described by Manabe and Stouffer (1988). The MSB calculations are for a 0.8 percent per year buildup of atmospheric CO_2; this choice is intended to include both the actual increase of CO_2 and that of other trace gases having a greenhouse effect. Here again the contribution from the shallow sound channel in the high southern latitudes is predominant. There is remarkably more warming over the Pacific path than the Atlantic path. Much of this difference can be attributed to the larger warming south of Australia as compared to south of Africa. MSB have also computed the warming for the path Heard to San

TABLE 1. Computed estimates of greenhouse warming along the Heard to Bermuda and Heard to Coos Bay refracted ray paths (Fig. 5), averaged along 3 Mm sections. The Hoffert (1980) warming is for the year 2000, based on the CO_2 scenario of Wuebbles, et al., (1984); the variation along the path is the result entirely of the change in depth of the sound axis. The MSB (Manabe, Spelman and Bryan, personal communication) warming is based on a three-dimensional atmosphere–ocean model (Manabe and Stouffer 1988), forming the difference mean (1990 to 2000) − mean (1980 to 1990), and dividing by 10 (for the annual rate). The MSB calculations are for the combined greenhouse gases.

Heard to Bermuda						Heard to Coos Bay				
Mm	Latitude	Longitude	$\bar{z}_{axis}$ (m)	Hoffert (m°C yr^{-1})	MSB (m°C yr^{-1})	Mm	Latitude	Longitude	$\bar{z}_{axis}$ (m)	MSB (m°C yr^{-1})
0	53.2°S	73.1°E				0	53.2°S	73.1°E		
			134	11.0	18.3				164	49.8
3	50.0°S	29.4°E				3	54.4°S	119.4°E		
			594	2.5	−6.5				625	28.8
6	35.4°S	1.9°W				6	41.1°S	154.9°E		
			893	1.0	+4.3				774	−1.5
9	8.6°S	28.3°W				9	21.1°S	176.3°E		
			830	0.9	−0.3				661	1.8
12	5.6°N	39.4°W				12	01.1°N	167.7°W		
			941	0.4	+5.5				1027	4.5
15	26.3°N	57.7°W				15	23.0°N	151.4°W		
			1340	0.3	+7.0				1201	4.0
16	32.2°N	64.6°W				18.4	42.7°N	129.2°W		
Range-weighted mean				+3.0	+4.4	range-weighted mean				+14.6

Francisco (not shown), giving an average warming of 16.7 m °C yr^{-1}, similar to 14.6 m °C yr^{-1} for Heard to Coos Bay.

b. Direct measurements

Figure 7 shows a running mean of temperature anomaly at the Panulirus station, the site of the longest existing time series of oceanic temperature. Roemmich (1989) distinguishes between the apparent long-term warming by 0.1°C between 1960 and 1980 (5 m °C yr^{-1}) for depths below 1300 m and the larger fluctuation at shallower depths (to be discussed). The spatial scale of the deep warming is not known. Warming by 5 m °C yr^{-1} through a column of 1 km leads by thermal expansion to a rise in sea level by 1 mm yr^{-1}. The global rise in sea level from widely scattered tide gauges is also estimated at 1 or 2 mm yr^{-1}: sea level estimates suffer from the fact that vertical motions of the Earth's crust are generally larger than 1 mm yr^{-1} (Barnett 1983, 1984b). The comparison between the measured deep warming and the sea level rise suggests the possibility of a widespread deep warming of order 5 m °C yr^{-1}; this is consistent with the MSB model estimates.

At a typical sound channel temperature, sound speed increases by 4 m s^{-1} per 1°C temperature rise. A mean warming by 5 m °C yr^{-1} leads then to a reduction in acoustic travel time by 140 ms yr^{-1} for the 16 Mm transmission (1 ms = 0.001 s). The effect of salinity is less by an order of magnitude. Tomography measurements now provide travel time to 1 ms precision at Mm ranges (see Fig. 10), so this should be a measurable signal. But, as in most geophysical problems, the issue is not measurement precision, but whether the effect can be detected in the presence of ocean variability.

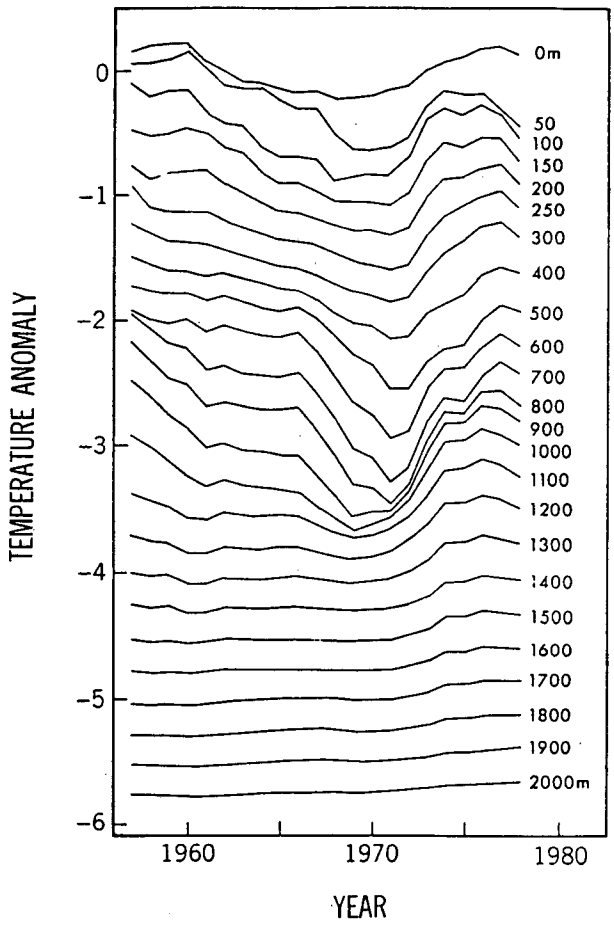

FIG. 7. The 5-year mean of temperature anomaly at the *Panulirus* station at 24 standard depths, according to Roemmich (1989). Standard depths are offset by 0.25°C. Roemmich distinguishes between the monotonic warming 1960–80 by 0.1°C beneath 1300 m, and the cold temperature pulse centered at 1972 above 1000 m.

5. Decadal variation

Returning now to Fig. 7, we note a decrease in temperature by 0.8°C centered at 1 km depth between 1958 and 1972, and a subsequent warming until 1978. A reoccupation of some IGY sections (Roemmich and Wunsch 1984) shows that the Bermuda anomaly extended over several megameters. Roemmich demonstrates a close resemblance between the steric sea level (as computed from changes in specific volume) and the sea level on nearby tide gauges. The 1958–72 cooling is associated with a sea level drop by 0.1 m. Compilations of tide gauge levels in the Atlantic and Pacific oceans indicate that decimeter fluctuations coherent over several years and with megameter scales are typical.

For the first time in oceanographic history there is now a sufficient database to make significant estimates of five to ten year changes in the temperature of the entire interior North Atlantic (Fig. 8). This figure compiled by Levitus (1989) shows a 15 year cooling in the Bermuda area by 0.8°C at 1 km depth, and extending over several Mm, in agreement with the Roemmich "point" estimate. The Bermuda anomaly averaged over the incoming ray path leads to a 600 ms change in travel time.

6. Mesoscale variation

At higher frequencies [2–10 cycles per year (cpy)] we can expect to find evidence for global mesoscale variability. A single mesoscale eddy with a mean temperature anomaly of 0.3°C extending over 100 km leads to a rms travel time departure of 60 ms. Treated as a random walk problem [Munk and Wunsch 1987, Eq. (58)], the rms departure increases as square-root of the range, in agreement with the observed 200 ms rms at 1 Mm. At 16 Mm we expect 800 ms rms variations in travel time.

Semtner and Chervin (1988) (hereafter SC) have developed a multilevel primitive-equation model which

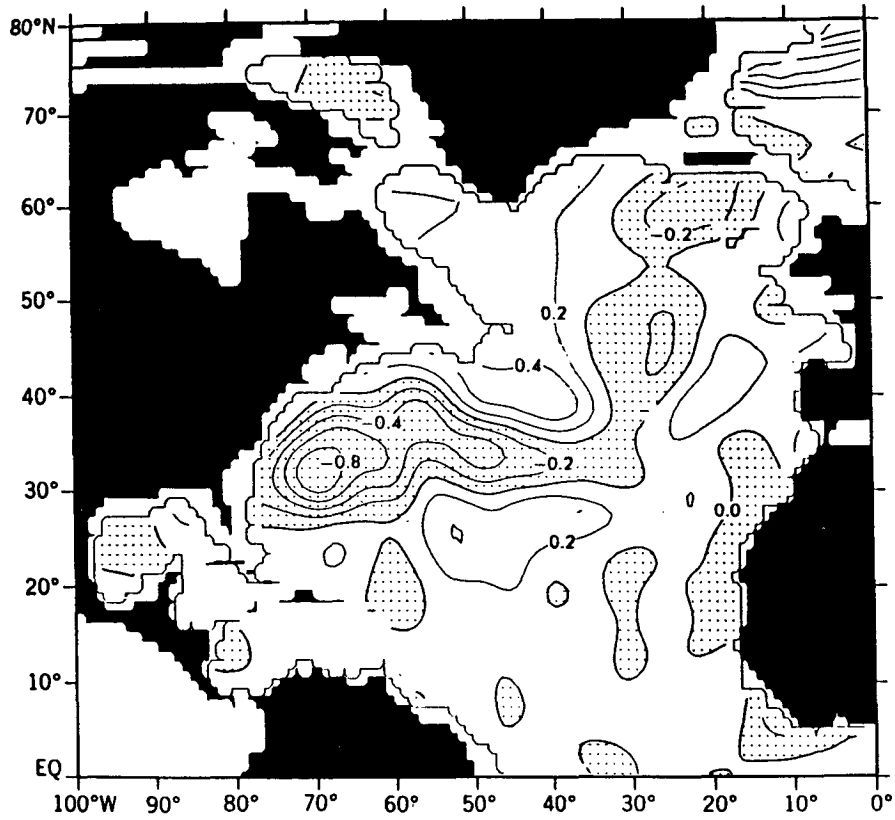

FIG. 8. Temperature anomaly (°C) (1970–74) relative to (1955–59) at 1000 m depth. (From Levitus 1989.)

exhibits global mesoscale variability. In the southern oceans the area of the Agulhas Current retroflection is marked by a high degree of spontaneous variability. Semtner (personal communication) has kindly furnished us time series of travel time along three axial-ray paths for years 19.5 to 22.0 of the SC model (Fig. 9). The variance is somewhat smaller than our random walk estimates. There is more fluctuation for the Bermuda path than for the two eastward paths, possibly as a result of passing through the Agulhas retroflection area. In Fig. 9, the SC results were detrended (to allow for what is presumably a numerical drift) and superposed on the MSB greenhouse warming estimates for 1990. If this procedure is of any merit, it suggests that global warming could be detected after 3 years along the eastward path, and after 10 years along the westward path. The display does not allow for the decadal variation.

In addition to these irregular variations of various scales, there is also a seasonal term. E. Maier-Reimer has kindly compiled the January minus July temperature difference along the Heard to Bermuda path, based on the Hamburg ocean general circulation model. The result is a travel time of 10 897 s for January versus 10 904 s for July. The travel time is less in January because of the warmer shallow temperatures in the Southern Hemisphere summer.

7. Acoustic transmission

The overall conclusion is that yearly mean travel times are subject to gyre-scale fluctuations of order 1 s, and that monthly mean travel times are subject to mesoscale fluctuations of similar magnitude. (But estimates of global ocean variability are themselves of great interest.) It will take a decade of scheduled acoustic transmissions to establish an underlying trend as-

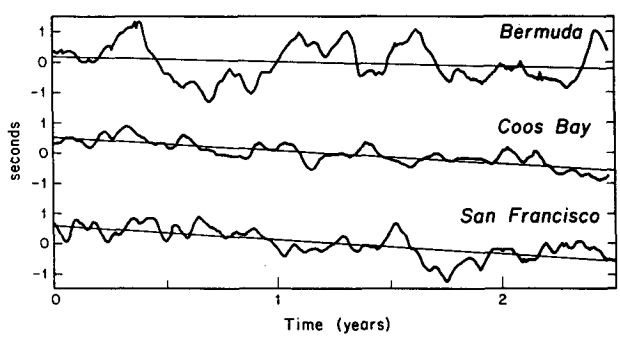

FIG. 9. Computer simulation of travel time variations along three ray paths. The mesoscale-induced fluctuation based on the model of Semtner and Chervin (1988) are superimposed on the greenhouse-induced trend in 1990 according to the model of Bryan, Manabe and Spelman (1988). The representation does not include gyre-scale variability.

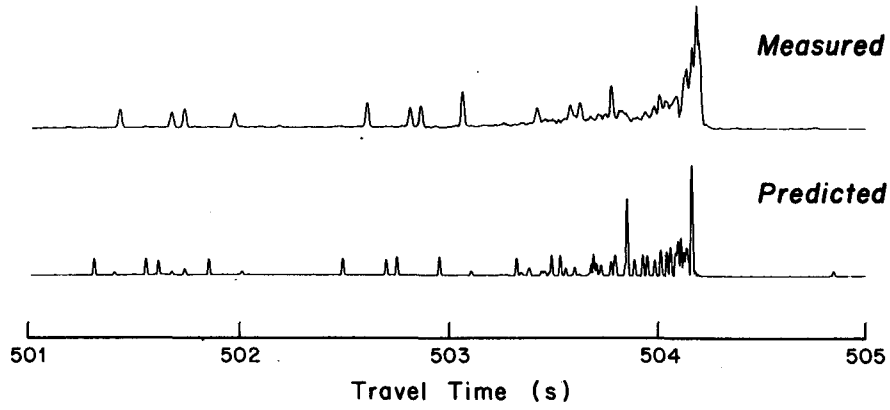

FIG. 10. Measured and predicted arrival pattern over 750 km range in the Reciprocal Transmission Experiment RTE87 in the Northeast Pacific. The pattern is typical of ranges of order 1 Mm. The plot is generated by forming the covariance of the measured signal with the phase-coded transmitted signal (Birdsall and Metzger 1986).

sociated with greenhouse warming. This speaks for a modern electrically driven source in place of the 1960 explosive source. Transmitters of adequate intensity and with the required frequency response now exist, and these are designed to operate at shallow depths. At the Heard Island site the sound axis is sufficiently shallow so that existing sources can be used without modification.

Figure 10 shows an arrival pattern typical of megameter ranges. The early individual peaks can be identified with known fairly steep ray arrivals, and the final sharp cutoff is associated with the near-axial flat propagation path. The ocean microstructure broadens an infinitely sharp transmitted pulse to roughly 10 ms at 1 Mm range. A source transmitting over a bandwidth of 100 Hz was chosen so that the resolution (e.g., the reciprocal bandwidth $1/100$ Hz $= 0.01$ s) roughly equals the 10 ms spreading. (A center frequency of 250 Hz proved convenient.) The arrival time of the centroid of a resolved feature can be measured to a precision of the spreading divided by

$$\sqrt{\text{signal/noise}},$$

or to 1 ms precision for a 100:1 (20 dB) S/N ratio.

For the 16 Mm transmission, the available frequency band width of 30 Hz is dictated by circumstances out of our control. An upper limit of about 70 Hz is determined by differential attenuation at higher frequencies, a lower limit of about 40 Hz by the increasing noise level at very low frequencies (Fig. 11). It is fortunate that an acoustic source of just by required frequency band is available. The resolution $1/(30)$ Hz $= 33$ ms is considerably sharper than the spreading which increases linearly with range [Flatté and Stoughton 1988, Eq. (22)] from 10 ms at 1 Mm to 160 ms at 16 Mm.

Table 2 is constructed by extrapolating to 16 Mm the 1 Mm tomographic transmissions using coded sources (Fig. 9), and coming up with a solution that is consistent with the 20 Mm transmissions from explosive sources (Fig. 1). The results are uncertain, and a feasibility experiment is called for. The proposed 209 dB source generates 6×10^3 W of acoustic power at peak frequency[3] (the cavitation limit at 100 m depth is 2×10^5 W); this gives 2×10^6 J during the coherence interval of 300 s (footnote d, Table 2). According to our estimates, the explosive source generated 3×10^7 J of low-frequency acoustic energy. One expects to make up for the weaker source level by avoiding shadowing and realizing a processing gain. The processing gain is achieved by transmitting a coded signal and correlating the received signal with a replica of the transmitted signal (see Table 2, footnote e on pulse compression).

With a single 209 dB source and a single receiver, the calculated S/N after processing is a comfortable 20 dB. By using a vertical array of sources and an array of receivers, this can be increased to 40 dB. (A high S/N is desirable for the feasibility experiment, as there is uncertainty whether the pulse compression can be achieved.) For a permanent station one would like to reduce the source level to 200 dB and concentrate on source reliability, and to make up for the weaker source by working with daily averages.

[3] This compares to 10^7 W for a large jet at take-off. The proposed site is 40 km from the nearest shore on Heard Island, where the spectral level of acoustic pressure is estimated at 102 dB re 1 μPa per Hz at the peak frequency; in the same units, porpoises generate up to 110 dB per Hz between 20 Hz and 200 Hz (Urick 1975, p. 194). Studies on acoustic seal deterrents (Shaughnessy et al. 1981) show that a 132 dB source is sufficient to annoy seals at very close range, but 185 dB may be reached before the sound becomes painful (Schusterman et al. 1972). Therefore a 209 dB source could annoy seals at 7 km range and become painful at 16 m range if it were used continuously for long periods.

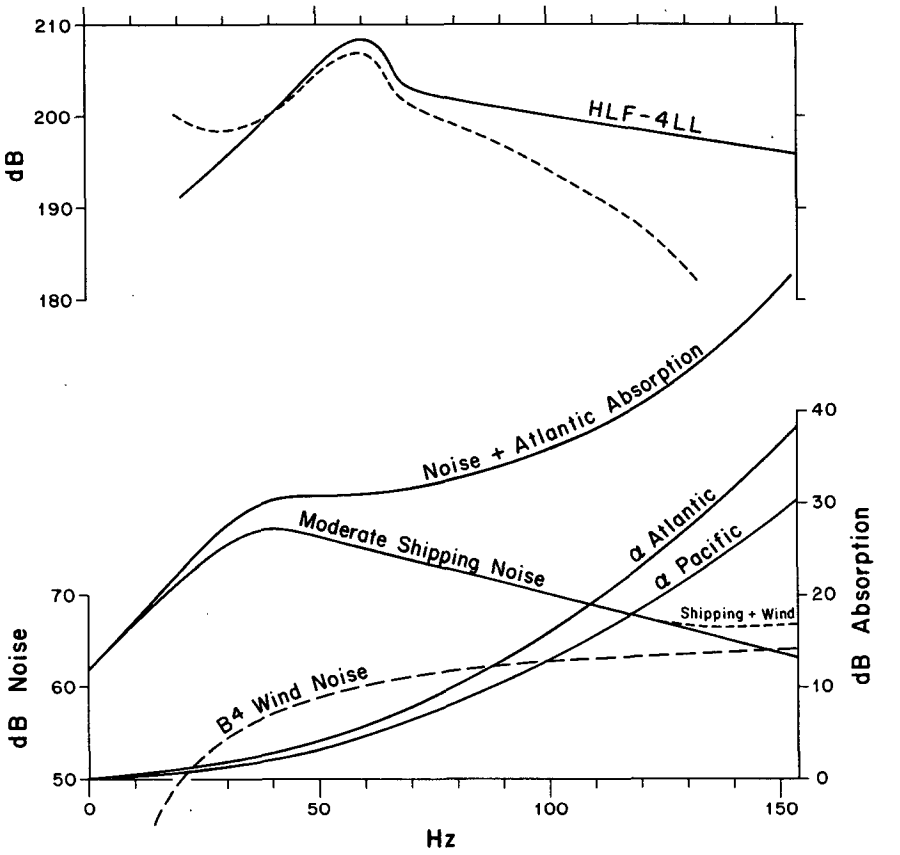

FIG. 11. Heard Source. Top solid curve shows the source level re 1 μPa at 1 m for the HLF-4LL source, peaked at 209 dB for 60 Hz. The effective spectral band is modified by two considerations: *absorption* shifts it towards lower frequency, and *noise* shifts it toward higher frequency. The two effects just about balance between 40 and 70 Hz. Absorption is computed for the Atlantic and Pacific for a 16 Mm range (Lovett 1980); it is dominated by a boron-borate relaxation process discovered by Yeager et al. (1973). Noise level is peaked at 40 Hz and equals 77 dB/Hz for moderate shipping; wind noise is negligible at the frequencies of interest. The effective spectrum (radiated energy minus noise minus absorption) is shown by the upper dashed curve on an arbitrary scale. The effective pass band is between 40 and 70 Hz.

We simply do not know what the arrival pattern is like at 16 Mm. Hopefully the sharp cutoff will survive, and possibly some stable arrival peaks.[4] Then with 20 dB S/N one ought to be able to measure travel time of these features to 10% of their width, or to 16 ms. For 40 dB, the precision is 1.6 ms. A 16 ms precision is adequate for our purposes.

8. Feasibility experiment

A feasibility experiment is planned for December 1990. The present plan provides for three HLF-4LL sources to be moored at about 150 m depth in 1000 m of water southeast of Heard Island. The sources are to be powered from an attending vessel. We foresee seven days of transmission, five days of a phase-coded sequence (maximal-linear-shift register) used in tomography experiments, and two days of CW at 53 Hz (this avoids confusions with existing 60 Hz and 50 Hz generating equipment). All this can be done with presently existing apparatus.

The experiment addresses two major uncertainties underlying global acoustic transmissions (their reality was established by the 1960 experiment): (i) whether the arrival pattern has sharp and stable features that can serve to determine the variable transmission time with 10 ms accuracy, and (ii) the required source strength for a permanent installation. It is desirable that the permanent source be under 200 dB, so that all the emphasis can be placed on reliable operation over long times. It is also desirable that the signal can

[4] Spiesberger et al. (1989) have monitored transmissions from Oahu, Hawaii to the coast of northern California at 4 Mm range! They propose a method for measuring changes in travel time by measuring changes in the average acoustic phase. This is potentially of greater accuracy than measuring the arrival time of individual amplitude features.

TABLE 2. Sonar equation.

	Pacific	Heard	Perth
(1) Range R	1 Mm	16 Mm	20 Mm
(2) Frequency $f \pm \frac{1}{2}\Delta f$	250 ± ½ 62.5 Hz	50 ± ½ 25 Hz	25 ± ½ 12.5 Hz[g]
(3) Source level	194 dB	209 dB	246 dB[h]
(4) Absorption	−4 dB	−6 dB	−1 dB
(5) Spreading			
Spherical to 10 km	−80 dB	−80	−80
Cylindrical to R	−20	−32	−33
Time Dispersion[a]	−15	−27	−28
Total (Spherical to R)[a]	−115 (−120)	−139 (−144)	−141 (−146)
Antipodal Convergence[b]		+6	+10
Shadowing[c]			−10
(6) Received signal level	+75 (70)	+70	+104
(7) Noise in 1 Hz band	68	75	78
in Δf band	86	89	89
(8) S/N unprocessed	−11 (−16) dB	−19 dB	+15 dB
(9) Pulse compression			
Coherence time Δt[d]	64 s (240 s)	300 s	
Processing gain[e]	36 dB	39 dB	
(10) S/N processed	+25 dB	+20 dB	+15 dB
(11) Array gain, 4 receivers	+4		0
(12) S/N processed for beam	+29 dB		+15
measured	+29 dB		+15
(13) Array gain, 3 sources[f]		+10 dB	
(14) Incoherent daily means[i]		+12 dB	

[a] Time spreading is taken proportional to R and inferred from the Perth-Bermuda transmission. The spreading is due to the increase with range of the time interval between the first (steep) and last (axial) arrivals. Time spreading is ignored in problems dealing with the *total* received energy. The combined spreading losses are generally 5 dB less than if spherical spreading is assumed throughout, and this is in accord with the measured intensity for the Pacific Triangle.

[b] Cylindrical spreading loss is approximately $10 \log(R_{AP} - R)$ instead of $10 \log R$, where $R_{AP} = 20$ Mm is the antipodal range. Internal wave diffusion generally limits antipodal convergence to 10 dB. This estimate is greatly in doubt for the scattered (diffused) Perth to Bermuda transmission.

[c] The estimate for shadowing loss is very uncertain.

[d] Internal wave decorrelation time $\sim f^{-1}R^{-1/2}$. Values follow from Flatté and Stoughton (1988) for near axial rays, and from some experimental results (Birdsall, personal communication). For the Pacific transmission, coherent processing for 64 s rather than 240 s was dictated by battery considerations. For the Heard transmission, the coherent processing time may have to be shortened to prevent overheating of source.

[e] $10 \log(\Delta t/\Delta f^{-1}) = 10 \log(\Delta t \cdot \Delta f)$ can be regarded as pulse compression from the coherent processing time Δt to the digit length Δf^{-1}, or alternatively as a consequence of the time bandwidth product.

[f] The gain is $20 \log N$, $10 \log N$ from beam forming and $10 \log N$ from additional power.

[g] The bubble frequency for 300 lbs of TNT at 1 km depth is 25 Hz (Urick 1975, Fig. 4.19A) and the bandwidth is from $0.75 f_b$ to $1.25 f_b$, or 12.5 Hz (Fig. 4.19B).

[h] The energy density E' for 300 lbs is 235 dB/Hz re $(1\ \mu\text{Pa})^2$ s (Fig. 4.19C), and $E = 235 + 10 \log\Delta f = 246$ dB re $(1\ \mu\text{Pa})^2$ s. This is equivalent to an energy density flux of 64 dB re 1 joule/m^2 (2.5×10^6 J m^{-2}) at a distance of 1 m, or $4\pi (2.5 \times 10^6) = 3.2 \times 10^7$ J (see Urick 1975 Fig. 4.18 and related discussion). The total energy of TNT is 10^3 cal/g = 6×10^8 for 300 lbs, so all but 5% goes into shock waves and heat.

[i] Using 5 log(1 day/300 s) in accordance with usual practice. A better procedure is to use 10 log for $S/N \gg 1$, and no gain for $S/N \ll 1$.

be received with single hydrophones or a very simple vertical array, thus enabling many oceanographic stations to participate.

9. Discussion

The widely held discussion of global warming derives largely from the results of a measuring program initiated by Keeling in 1957 (Keeling 1960), following the seminal proposal by Revelle and Suess (1957) that an increase in atmospheric CO_2 was taking place with important climatic implications, and that the rate of increase should be measurable even then with existing techniques. Keeling has documented an increase in atmospheric CO_2 from 315 to 350 ppmv over a 25 year period. Direct observational evidence for atmospheric and sea surface warming is not clear-cut. Model predictions have to allow properly for heat lost to the ocean to get the atmospheric warming right.

It is, of course, difficult to measure changes of order

10 m °C yr^{-1} by local soundings. Bretherton et al. (1984) have considered the feasibility of XBT surveys for measuring five-year changes in North Atlantic heat storage to an accuracy equivalent to ±10 W m^{-2} (greenhouse doubling amounts to +4 W m^{-2}). The requirement is for 600 XBTs launched annually from ships along seven properly spaced tracks.

The TOPEX/POSEIDON altimetric satellite is expected to yield global mean sea level with an accuracy of 10 or 20 mm during the 3 to 5 year duration of the mission (Born et al. 1986). This implies that the mission could barely detect a sea level rise by 2 mm yr^{-1}, the estimated present rate. By comparison, acoustic travel times could measure the rate of warming associated with a thermal expansion of the ocean column by 2 mm yr^{-1}. Thermal expansion associated with 4 W m^{-2} yields roughly 6 mm yr^{-1}.

The extraordinary transmission characteristics of sound in the ocean offer an opportunity for measuring ocean temperature changes on a large scale. Such measurements, if successful, will serve two principal purposes: (i) they can provide early warning of an upper ocean warming in the southern oceans and of the interior warming in other ocean basins, and (ii) they can be assimilated into computer simulations and thus provide some control over the prediction scenarios. A multiplicity of receivers should allow separate estimates for the different ocean basins. For example, the New Zealand receiver yields an estimate of warming in the Southern Ocean. A comparison with the Tahiti travel times yields some additional information of warming in the South Pacific (but at greater depth), and a further comparison with the San Francisco record gives information on warming in the North Pacific. But the information is not adequate for an inversion of travel time data to yield the global distribution in ocean warming. Multiple sources and receivers strategically located might permit the application of inverse methods (as in Ocean Acoustic Tomography).

In the event that questions concerning the intensity and character of the arrival sequence of global acoustic transmissions are successfully resolved by the feasibility experiment, there remain problems concerning the interpretation of travel time changes in terms of various ocean processes, among them greenhouse warming, gyre scale and mesoscale variability. To resolve the ambiguities will require many receivers and at least a decade of recording. There is also the problem of changes in travel time associated with changes in the path rather than with changes in temperature along the (undisturbed) path. This problem has plagued the interpretation of tomographic experiments since their very inception (Mercer and Booker 1983). But here it must be remembered that a travel time along a Fermat minimum ray path is, to first order, invariable with path changes, so that the corrections are of second order. (Munk and Wunsch 1985, §1; this will be discussed in a forthcoming note.) The quadratic bias is such that travel time through a structured ocean is generally less than through a smooth ocean with the same mean properties (Munk and Wunsch 1987). But what counts here is not the existing warm bias associated with ocean structure, but a secular change in warm bias; still, diminishing travel times cannot distinguish between an ocean of increasing refractive complexity and one with increasing temperature.

There is, of course, considerable uncertainty concerning the rate and distribution of greenhouse warming, and of the estimates of the associated rate of decrease in acoustic travel times. In our view this uncertainty is a reason for making the measurements, not an argument against it.

The site south of Heard Island has access to all of the major ocean basins, the North and South Atlantic, the North and South Pacific, the Indian Ocean and adjoining sector of the Southern Ocean. It is the most ambitious site, and it was chosen deliberately to bracket the problem of what can be done with global ocean temperature soundings.

Acknowledgments. Our interest in long-range acoustic transmission is a direct consequence of the work on ocean acoustic tomography supported by the Office of Naval Research and the National Science Foundation. A. Forbes was supported by a grant from the Secretary of the Navy Research Chair in Oceanography held by W.M. We are indebted to Peter Worcester, Tim Barnett, Kirk Bryan, Ted Birdsall, Syd Levitus for critical discussions. We thank W. C. O'Reilly and Don Betts for help with the construction of the diagrams, and Jane Di Tullio for preparing the manuscript.

REFERENCES

Barnett, T. P., 1984a: Long-term trends in surface temperature over the oceans. *Mon. Wea. Rev.*, **112**, 303–312.

——, 1984b: The estimation of "Global" sea level change: A problem in uniqueness. *J. Geophyhs. Res.*, **89**, 7980–7988.

——, and Schlesinger M., 1988: Detecting changes in global climate induced by greenhouse gases. *J. Geophys. Res.*, **92**, 14 772–14 780.

Birdsall, T., and K. Metzger Jr., 1986: Factor inverse matched filtering. *J. Acoust. Soc. Amer.*, **79**, 91–99.

Born, G. H., B. D. Tapley, J. C. Ries and R. H. Stewart, 1986: Accurate measurements of mean sea level changes by Altimetric Satellites. *J. Geophys. Res.*, **91**, 11 775–11 782.

Bretherton, F. P., M. J. McPhaden and E. B. Kraus, 1984: Design studies for climatological measurements of heat storage. *J. Phys. Oceanogr.*, **14**, 318–337.

Bryan, K., S. Manabe and M. J. Spelman, 1988: Interhemispheric asymmetry in the transient response of a coupled ocean-atmosphere model to a CO_2 forcing. *J. Phys. Oceanogr.*, **18**, 851–867.

Dashen, R., and W. Munk, 1984: Three models of global ocean noise. *J. Acoust. Soc. Amer.*, **76**, 540–554.

Flatté, S., and R. Stoughton, 1988: Predictions of internal-wave effects on the ocean acoustic coherence, travel-time variance, and intensity moments for very long-range propagation. *J. Acoust. Soc. Amer.*, **84**, 1414–1424.

Folland, C. K., and D. E. Parker, 1988: Comparison of corrected sea surface and air temperature for the globe and the hemispheres,

1856–1988. *13th Annual Climate Diagnostics Workshop,* Boston, 1–3.

Gornitz, V., and S. Lebedeff, 1987: Global sea-level changes during the past century. *Sea-level change and coastal evolution.* D. Nummedal, O. H. Pilkey and J. D. Howard, Eds., Society of Economic Paleontologists and Mineralogists, Special Publication No. **41,** 3–16.

Hoffert, M. I., A. J. Callegari and C. T. Hsieh, 1980: The role of deep sea heat storage in the secular response to climatic forcing. *J. Geophys. Res.,* **85,** 6667–6679.

Keeling, C. D., 1960: The concentration and isotopic abundances of carbon dioxide in the atmosphere. *Tellus,* **12,** 200–203.

——, A. F. Carter and W. G. Mook, 1984: Seasonal, latitudinal and secular variations in the abundance and isotopic ratio of atmospheric CO_2. II: Results from oceanographic cruises in the tropical Pacific Ocean. *J. Geophys. Res.,* **89,** 4615–4628.

Kibblewhite, A. C., R. N. Denham and P. H. Barker, 1966: Long-range sound-propagation study in the Southern Ocean—Project Neptune. *J. Acoust. Soc. Amer.,* **38,** 629–643.

Knox, R. A., 1989: Ocean Acoustic Tomography: A Primer. NATO Advanced Study Institute. *Modelling the Ocean General Circulation and Geochemical Tracer Transport,* D. Reidel.

Levitus, S., 1989: Inter-pentadal variability of temperature and salinity of intermediate depths of the North Atlantic (1970–74) versus (1955–59). *J. Geophys. Res. (Oceans),* in press.

Lovett, J., 1980: Geographic variation of low-frequency sound absorption in the Atlantic, Indian and Pacific Oceans. *J. Acoust. Soc. Am.,* **67,** 338–340.

MacCracken, M. C., and F. M. Luther, 1985: Projecting the climatic effects of increasing carbon dioxide. United States Department of Energy, DOE/ER-0237, 38 pp.

Manabe, S., and R. J. Stouffer, 1988: Two stable equilibria of a coupled ocean–atmosphere model. *J. Climate,* **1,** 841–866.

Mercer, J. A., and J. R. Booker, 1983: Long-range propagation of sound through oceanic mesoscale structures. *J. Geophys. Res.,* **88,** 689–699.

Mook, W. G., M. Koopmans, A. F. Carter and C. D. Keeling, 1983: Seasonal, latitudinal and secular variations in the abundance and isotopic ratio of atmospheric CO_2. I: Results from land stations. *J. Geophys. Res.,* **88,** 10 915–10 933.

Munk, W., and C. Wunsch, 1982: Observing the ocean in the 1990's. *Phil. Trans. Roy. Soc. London,* **307,** 439–464.

——, and ——, 1985: Biases and caustics in long-range acoustic tomography. *Deep-Sea Res.,* **32,** 1317–1346.

——, and ——, 1987: Bias in acoustic travel time through an ocean with adiabatic range-dependence. *Geophys. Astrophys. Fluid Dyn.,* **39,** 1–24.

——, and P. F. Worcester, 1988: Ocean acoustic tomography. *Oceanography,* **1,** 8–10.

——, W. C. O'Reilly and J. L. Reid, 1988: Australia-Bermuda sound transmission experiment (1960) revisited. *J. Phys. Oceanogr.,* **18,** 1876–1898.

Roemmich D., 1989: Sea level and the thermal variability of the ocean. Chapter 1. NRC study on Sea Level, R. Revelle, Chairman.

——, and C. Wunsch, 1984: Apparent changes in the climatic state of the deep North Atlantic Ocean. *Nature,* **307,** 447–450.

Schlesinger, M. E., 1986: Equilibrium and transient climatic warming induced by increased atmospheric CO_2. *Clim. Dyn.,* **1,** 35–51.

——, and Jiang Xingjian, 1988: The transport of CO_2-induced warming into the ocean: An analysis of simulations by the OSU coupled atmosphere-ocean general circulation model. *Clim. Dyn.,* **3,** 1–17.

Schusterman, R. J., R. F. Balliet and J. Nixon, 1972: Underwater audiogram of the California Sea Lion by the Conditioned Vocalization Technique. *J. Exp. Anal. Behav.,* **17,** 339–350.

Semtner, A. J., and R. M. Chervin, 1988: A simulation of the global ocean circulation with resolved eddies. *J. Geophys. Res.,* **93,** 15 502–15 522.

Shaughnessy, P. D., A. Slemmelink, J. Cooper and P. G. H. Frost, 1981: Attempts to develop acoustic methods of keeping Cape Fur Seals *Arctocephalus Pusillus* from fishing nets. *Biol. Cons.,* **21,** 141–158.

Shockley, R. C., J. Northrop, P. G. Hansen and C. Hartdegen, 1982: SOFAR propagation paths from Australia to Bermuda: Comparison of signal speed algorithms and experiments. *J. Acoust. Soc. Amer.,* **71:1,** 51–60.

Spiesberger, J. L., P. J. Bushong, K. Metzger, Jr. and T. G. Birdsall, 1989: Ocean acoustic tomography: Estimating the acoustic travel time with phase. *IEEE J. Oceanic Eng.,* **14,** 108–119.

Spindel, R. C., and J. L. Spiesberger, 1981: Multipath variability due to the Gulf Stream. *J. Acoust. Soc. Amer.,* **19,** 982–988.

Urick, R. J., 1975: *Principles of Underwater Sound,* McGraw-Hill, 384 pp.

Wuebbles, D. J., M. C. MacCracken and F. M. Luther, 1984: A proposed reference set of scenarios for radiatively active constituents. United States Department of Energy, Washington, DC, (DOE/NBB-0066). [Available from NTIS, Springfield, Virginia.]

Yeager, E., F. Fisher, J. Miceli and R. Bressel, 1973: Origin of the low frequency sound absorption in sea water. *J. Acoust. Soc. Am.,* **53,** 1705.